Interstrand Cross-Link Induction by UV Radiation in Bromodeoxyuridine-Substituted DNA: Dependence on DNA Conformation†

Sylvain Cecchini, Christel Masson, Carole La Madeleine, Michael A. Huels, Léon Sanche, J. Richard Wagner, and Darel J. Hunting*

Center for Research in Radiology (CR2), Department of Nuclear Medicine and Radiobiology, Faculty of Medicine, Université de Sherbrooke, Québec, Canada J1H 5N4

Received April 29, 2005; Revised Manuscript Received September 6, 2005

ABSTRACT: DNA interstrand cross-links (ICL) can be induced both by natural products (e.g., psoralens with UVA) and by chemical agents, some of which are used in chemotherapy (e.g., Carboplatin and mitomycin C). Here, we report the formation of ICL by UV radiation in brominated DNA, but only for very specific conformations. The quantum yields for strand break and cross-link formation depend on the wavelength with a maximum near 280 nm. It is known that the photosensitization of DNA by bromodeoxyuridine (BrdUrd) results mainly from the electron affinity of bromine, leading to the irreversible formation of 2′-deoxyuridin-5-yl radicals (dUrd•) upon the addition of an electron from an adjacent adenosine. It is well documented that the photolytic loss of the bromine atom is greatly suppressed in single-stranded DNA versus that in double-stranded DNA. To study this behavior, we have used two models of BrdUrd-mediated sensitization: one consists of a DNA duplex containing a bulge, formed by five mismatched bases, including the BrdUrd, and the other consists of completely duplex DNA. UV irradiation induces much higher levels of single-strand breaks (ssb) in the completely duplex DNA at the BrdUrd site compared to the DNA with a bulge. However, in completely duplex DNA, ssb appear only in the brominated strand, whereas in the bulged duplex DNA, ssb occur on *both* strands. Most importantly, we also observe formation of interstrand cross-links in bulged duplex DNA in the BrdUrd region. Thus, we propose that UV irradiation of cells containing BrdUrd incorporated randomly into duplex DNA will create many ssb, whereas BrdUrd present in DNA bulges or open regions in double-stranded DNA (transcription bubbles, replication forks) will lead to potentially lethal damage in both strands in the form of ICL. These findings may help explain the potent clinical antiviral activity of IdUrd and BrdUrd (e.g., IdUrd is used to treat eye infections caused by the herpes virus) and suggest that ICL formation may be a very specific probe for identifying single-stranded regions in the DNA of living cells. In addition, this model system provides an excellent means of introducing ICL for studies on their repair and biological consequences.

ICL[1] repair in cells involves both DNA excision repair and recombination, thus increasing the complexity of the repair process (*1*−*3*). Studies on Fanconi anemia, a rare autosomal recessive disorder characterized by sensitivity to ICL agents, have identified seven FA genes involved in cell cycle checkpoints and DNA repair (*4*−*6*). Very early studies demonstrated that UVB and UVC can induce intrastrand dimers between two pyrimidines on the same strand, but more recently, Kypr's group has shown that UVC light can induce cross-links between the complementary strands of DNA without external chemical agents (*7*−*9*). Cadet's group has found that the production of these interstrand cross-links is induced by UVC photolysis of dry, A-form DNA (*10*). In the study presented here, we report the conformation-dependent induction of interstrand cross-links in brominated B-DNA by UV irradiation. Studies over the past 40 years have demonstrated that 5-bromo-2′-deoxyuridine (BrdUrd) is able to radiosensitize (*11*−*14*) and photosensitize cells (*15*−*17*). Recent studies have demonstrated that BrdUrd is a type I photosensitizer characterized by electron transfer from a nearby adenine to BrdUrd (*18*). The bromine anion is rapidly ejected, leaving two reactive species in DNA, the uracil-5-yl radical and an adenine radical cation. The mechanism of radical stabilization is still under investigation; however, Wang and Zeng, working with short oligonucleotides containing a brominated cytosine, have recently found

† This work was supported by the National Cancer Institute of Canada.

* To whom correspondence should be addressed. Telephone: (819) 346-1110, ext. 14604. Fax: (819) 564-5442. E-mail: darel.hunting@usherbrooke.ca.

[1] Abbreviations: A, adenine; AB, bromodeoxyuridine-substituted oligonucleotide 1; AT, non-bromodeoxyuridine-substituted oligonucleotide 2; B, 5-bromouracil; BrdUrd, 5-bromo-2′-deoxyuridine; C, cytosine; C^{BR}, 5-bromocytosine; CC, semicomplementary oligonucleotide 4; DSc, complementary double strand; DSsc, semicomplementary double strand; $dUrd^-$, 2′-deoxyuridine-yl anion; dUrd•, 2′-deoxyuridine-yl radical; e_{aq}^-, hydrated electron; EDTA, ethylenediaminetetraacetic acid; FdUrd, 5-fluoro-2′-deoxyuridine; G, guanine; ICL, interstrand cross-link; IdUrd, 5-iodo-2′-deoxyuridine; $O_2^{\bullet -}$, superoxide radical; •OH, hydroxyl radical; PAGE, polyacrylamide gel electrophoresis; T, thymine; TA, complementary oligonucleotide 3; UVA, ultraviolet A radiation; UVB, ultraviolet B radiation; UVC, ultraviolet C radiation; Hg−Xe, mercury−xenon; $E_?$, photon energy; R, relaxed circular form of pGEM plasmid; ss-pGEM, nicked pGEM plasmid; ICL-pGEM, interstrand cross-link of the pGEM plasmid; dGuo, 2′-deoxyguanosine; dAdo, 2′-deoxyadenosine.

10.1021/bi050799x CCC: $30.25
Published on Web 12/02/2005

Composition	Strand #	*Title and sequence*	Abbreviation
oligonucleotide 1/3:		Brominated complementary double stranded oligonucleotide	$DSc_{1/3}$-AB//TA
1 Brominated strand	**1**	5'-C-G-A-G-T-A-C-T-G-C-A-A-**B**-A-A-C-G-T-G-T-A-C-A-G-C-3'	SS_1-AB
3 Complementary strand	**3**	3'-G-C-T-C-A-T-G-A-C-G-T-T- A -T-T-G-C-A-C-A-C-G-T-C-G-5'	SS_3-TA
oligonucleotide 1/4:		Brominated semi-complementary double stranded oligonucleotide	$DSsc_{1/4}$-AB//CC
1 Brominated strand	**1**	5'-C-G-A-G-T-A-C-T-G-C-A-A-**B**-A-A-C-G-T-G-T-A-C-A-G-C-3'	SS_1-AB
4 Semi-complementary strand	**4**	3'-G-C-T-C-A-T-G-A-C-G-C-C-C-C-C-G-C-A-C-A-C-G-T-C-G-5'	SS_4-CC
		Brominated single stranded region	
oligonucleotide 2/3:		Non brominated complementary double stranded oligonucleotide	$DSc_{2/3}$-AT//TA
2 Non brominated strand	**2**	5'-C-G-A-G-T-A-C-T-G-C-A-A-T-A-A-C-G-T-G-T-A-C-A-G-C-3'	SS_2-AT
3 Complementary strand	**3**	3'-G-C-T-C-A-T-G-A-C-G-T-T- A -T-T-G-C-A-C-A-C-G-T-C-G-5'	SS_3-TA
oligonucleotide 2/4:		Non brominated semi-complementary double stranded oligonucleotide	$DSsc_{2/4}$-AT//CC
2 Non brominated strand	**2**	5'-C-G-A-G-T-A-C-T-G-C-A-A-T-A-A-C-G-T-G-T-A-C-A-G-C-3'	SS_2-AT
4 Semi-complementary strand	**4**	3'-G-C-T-C-A-T-G-A-C-G-C-C-C-C-C-G-C-A-C-A-C-G-T-C-G-5'	SS_4-CC

B :bromodeoxyuracil; T : thymine; A : adenine; G : guanine; C : cytosine; SS : single strand; DS : double strand; c :complementary; sc :semi-complementary (bulge).

FIGURE 1: Sequences of brominated (strand 1), nonbrominated (strand 2), complementary (strand 3), and semicomplementary (strand 4) oligonucleotides showing the location of the single-stranded bubble (double strand 1/4 and 2/4) and the position of the bromodeoxyuridine (B).

that the mechanism of stabilization may involve the formation of a bond between two radical species creating an intrastrand cross-link between CBr and G (*19*).

In this study, we report that UV radiation-induced ICL are produced most intensively in the single-stranded brominated bulge region of a double-stranded oligonucleotide. In contrast, the production of strand breaks is much more pronounced with brominated, completely double-stranded DNA but occurs exclusively in the brominated strand. Interestingly, with a brominated double-stranded DNA containing a bulge, strand breaks are generated, albeit at a much lower frequency, in both the brominated and nonbrominated strands within the bubble region.

MATERIALS AND METHODS

Oligonucleotide Studies

Labeling the Oligonucleotides at the 5′ End. The oligonucleotides shown in Figure 1 were purchased from the DNA Synthesis Lab (University of Calgary, Calgary, AB). [γ-^{32}P]-ATP (111 TBq/mmol) and T4 polynucleotide kinase (Amersham Pharmacia Biotech, Piscataway, NJ) were used for end-labeling oligonucleotides, which were then purified on a G50 Sephadex microcolumn, yielding a labeled oligonucleotide which was more than 99.9% [γ-^{32}P]ATP free. For each experiment, 100 pmol of oligonucleotide was labeled, and approximately 75% of the end-labeled oligonucleotide was recovered after purification on a G50 column.

Hybridization of Oligonucleotides. Hybridization of oligonucleotides with their complementary or semicomplementary strand was performed in 60 μL of solution, using a 2-fold excess of the nonradioactive strand. Solutions were heated to 80 °C for 5 min and then allowed to cool slowly (2 h) to room temperature.

Verification of Hybridization. To determine the extent of hybridization for radioactive oligonucleotides with or without a mismatched bubble, samples were separated by electrophoresis in a nondenaturing polyacrylamide gel. Figure 2 shows the migration of single-stranded oligonucleotides SS_1-AB* and SS_2-AT* (lanes 1 and 4, respectively) which migrate faster than double-stranded oligonucleotides (lanes 2, 3, 5, and 6). The asterisk indicates the radioactive strand. Complementary (lanes 2 and 5, oligonucleotides $DSc_{1/3}$-AB*//TA and $DSc_{2/3}$-AT*//TA, respectively) and semicomplementary (lanes 3 and 6, oligonucleotides $DSsc_{1/4}$-AB*//CC and $DSsc_{2/4}$-AT*//CC, respectively) both migrate at approximately the same rate (*20*). Thus, complete hybridization of labeled oligonucleotides with their complementary and semicomplementary strands occurs under our conditions.

Strand Break and Interstrand Cross-Link Detection and Quantification. Denaturing PAGE gel electrophoresis was used to detect interstrand cross-links, as previously described

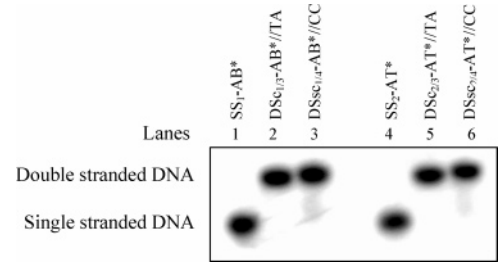

FIGURE 2: Nondenaturing gel electrophoresis of hybridized ^{32}P-labeled oligonucleotides: lanes 1 and 4, single-stranded oligonucleotides 1* (SS_1-AB*) and 2* (SS_2-AT*), respectively; lanes 2 and 3, hybridized oligonucleotides 1* and 3 ($DSc_{1/3}$-AB*//TA) and 1* and 4* ($DSsc_{1/4}$-AB*//CC), respectively (bubble); and lanes 5 and 6, hybridized oligonucleotides 2* and 3 ($DSc_{2/3}$-AT*//TA) and 2* and 4 ($DSsc_{2/4}$-AT*//CC), respectively (bubble). The asterisk indicates the ^{32}P end-labeled strand.

(*21*−*23*). Following UV irradiation, samples were loaded on a 7 M urea denaturing 20% polyacrylamide gel (35 cm × 43 cm) and electrophoresed for 2 h at 30 W. A phosphorescent screen was exposed to the gel overnight (12 h) and subsequently analyzed with a fluorescence scanning system, Storm (Molecular Dynamics Inc.), using a 100 μm pixel size. The gels were quantified using ImageQuant version 5.0 (Molecular Dynamics Inc.). Molecular weight ladders were generated by random depurination using formic acid at room temperature followed by cleavage at apurinic sites with piperidine at 90 °C.

Plasmid Studies

Plasmid and Bacteria. Plasmid PGEM-3Zf(−) (3197 bp, Promega) is a pUC derivative. Supercoiled plasmid was isolated from *Escherichia coli* strain 4203 (Rec A$^-$) using a Qiagen extraction kit.

Media and Growth Conditions. Bacterial cultures were grown at 37 °C in minimal medium (medium A) containing appropriate supplements: 1 mM $MgSO_4 \cdot 7H_2O$, 0.2% glycerol, 0.5 mg/mL vitamin B_1, 0.1% casamino acids, and 1.25 mM deoxyadenosine. The BrdUrd medium was supplemented with 1.25 μg/mL BrdUrd and 0.5 μg/mL thymidine. The thymidine medium was supplemented with 0.5 mg/mL thymidine. The BrdUrd incorporation ratio in plasmid PGEM-3Zf(−) was determined by HPLC with UV detection (Waters, Milford, MA) using a reversed phase column (Waters C18 ODS-AQ, 4.6 nm × 250 nm). The mobile phase was a 50 mM aqueous solution of potassium dihydrogen phosphate (pH 5.5) and 8% methanol.

Plasmid Strand Breaks. Agarose gel electrophoresis and SYBR Green I staining (Molecular Probes) were used to detect single- and double-strand breaks in the plasmid DNA as described by Martin et al. (*24*). After UV irradiation, samples were loaded on a 1% agarose gel (35 cm × 43 cm) and electrophoresed for 1 h at 70 V. Following staining, samples were analyzed with a fluorescence scanning system at 450 nm, using a 100 μm pixel size (Storm, Molecular Dynamics Inc.). The gel bands were quantified using ImageQuant version 5.0 (Molecular Dynamics Inc.).

Plasmid Interstrand Cross-Links. To quantify ICL formation in plasmid DNA during UV irradiation, the alkaline electrophoretic assay method (*25*) was used. After UV irradiation, closed-circular PGEM-3Zf(−) was linearized with *Hin*dIII, then dephosphorylated with antarctic phosphatase (Biolabs) at 5 units/μL, and finally labeled at the 5′ end using [γ-^{32}P]ATP and polynucleotide kinase (see Labeling of Oligonucleotides at the 5′ End above). Labeled DNA was separated by alkaline agarose gel electrophoresis at 3.5 V/cm for 8 h, after which a phosphorescent screen was exposed to the gel overnight (12 h) and analyzed with the Storm laser scanner using a 100 μm pixel size. The gel was quantified using ImageQuant version 5.0 (Molecular Dynamics).

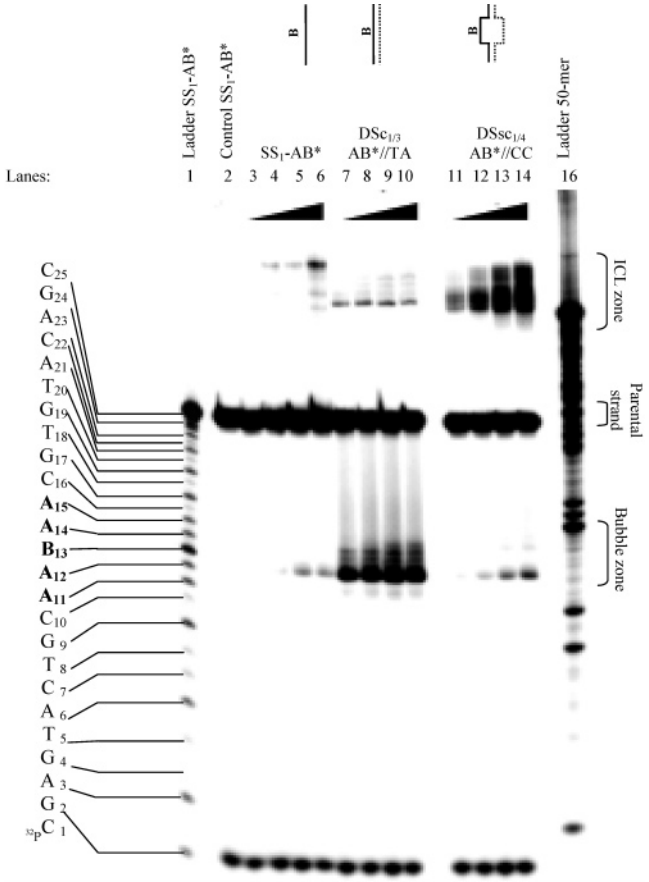

FIGURE 3: Formation of single-strand breaks and interstrand cross-links in bromodeoxyuridine-photosensitized oligonucleotides. Oligonucleotides were photolyzed with different doses of UVB under a nitrogen atmosphere, and damage in single-stranded (SS_1-AB*), double-stranded ($DSc_{1/3}$-AB*//TA), or double-stranded with a single-stranded bubble ($DSsc_{1/4}$-AB*//CC) (nucleotides 11−15 mismatched) was assessed. The asterisk indicates the ^{32}P-labeled strand. In this experiment, the strand containing a BrdUrd (oligonucleotide SS_1-AB) at position 13 was labeled with ^{32}P.

Experimental Conditions

Bubbling with Nitrogen. To minimize residual dissolved gases that could interact with radicals, oligonucleotide solutions were bubbled with wet nitrogen gas having a stated purity of 99.998% during UV irradiation with a 1000 W lamp.

UV Photolysis. Two methods of photolysis were used in this study. For UVB studies, we used a transilluminator (Spectroline) with a UVB fluence of 1.3 kJ m^2 min^{-1}. To remove residual UVC light, we used a homemade pyridine filter, which blocked 50% of the light at 316 nm and 99.9% of the light below 290 nm (data not shown). For studies with monochromatic light, we used a 1000 W Hg−Xe arc lamp (Spectra-Physics, Oriel Instruments, Stratford, CT) fitted with an infrared filter and monochromator with an adjustable

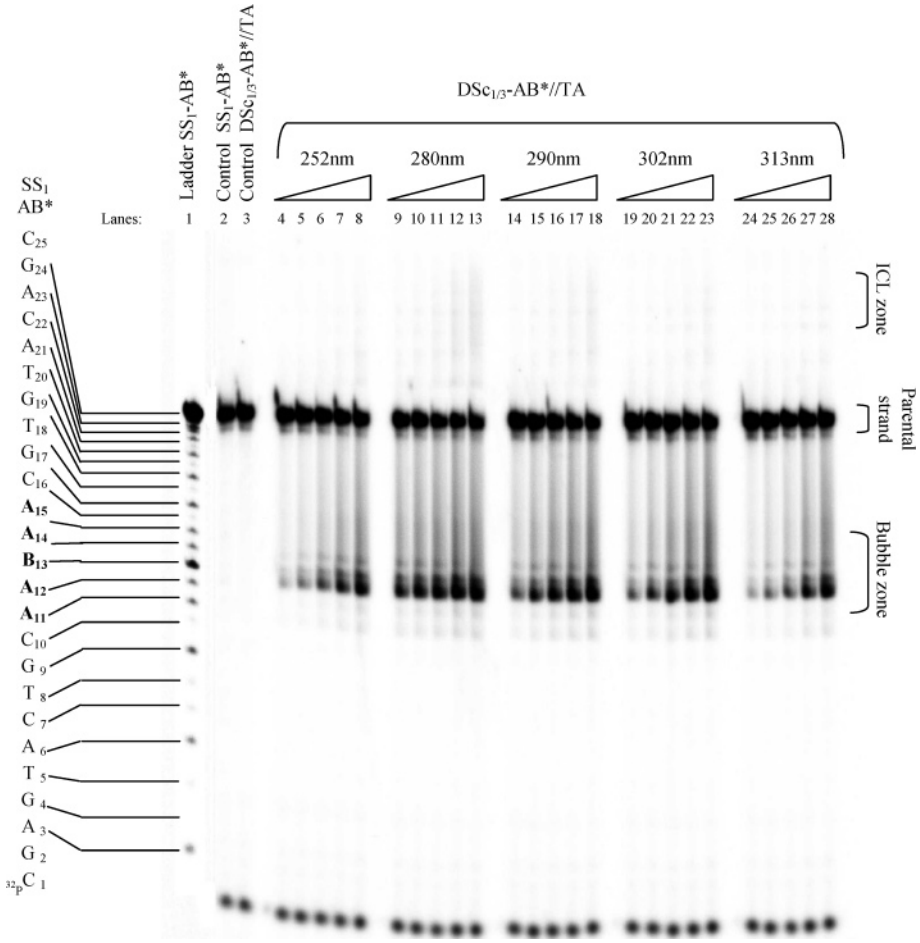

FIGURE 4: Formation of single-strand breaks and interstrand cross-links in bromodeoxyuridine-sensitized oligonucleotides. Oligonucleotides were UV-irradiated with different wavelengths and doses: 252 nm (200; 400; 800; 1600; 3200 J/m^2); 280 nm (3100, 6300, 12500; 25100; 50200 J/m^2); 290 nm (3500, 7100, 14,100; 28300; 56600 J/m^2); 302 nm (5,700; 11,400; 22,850; 45,600; 91,200 J/m^2); 313 nm (11,600; 23,200; 46,300; 92,700; 185,400 J/m^2) under a nitrogen atmosphere, and damage in completely double-stranded DNA (DSc_{13}-AB*//TA) was assessed. The asterisk indicates the ^{32}P-labeled strand. In this experiment, the strand containing a BrdUrd (oligonucleotide SS_1-AB) at position 13 was labeled with ^{32}P.

wavelength grating (Spectral Energy Corp., Washingtonville, NY). The wavelength accuracy of the monochromator was ±0.5 nm, and the energy width was set at ±2.5 nm. The photon fluence rate at each wavelength was measured with a 3M Photodyne Optical Mini Meter (Opticon Inc.).

Calculation of Quantum Yields for Interstrand Cross-Link and Strand Break Production. The following formula was used to calculate the quantum yield for each lesion:

$$\text{quantum yield} = \frac{(\text{percent of the band measured in the gel} \times 75\ \text{pmol of oligonucleotide})}{[\text{fluence} \times E_{\lambda}(\text{photon}) \times (100 - \text{transmittance}) \times \text{size of the target}]}$$

RESULTS

UVB Induced Breaks and Cross-Links Involving the Brominated Strand in Complementary or Semicomplementary Double-Stranded DNA (Figure 3). As shown in Figure 3, the presence of bromodeoxyuridine at position 13 sensitized very slightly the single-stranded oligonucleotide, SS_1-AB*, to UVB radiation-induced breakage (lanes 3−6). In contrast, the presence of bromodeoxyuridine in completely complementary duplex DNA ($DBc_{1/3}$-AB*//TA, lanes 7−10) greatly enhanced strand break formation 5′ of the BrdUrd. When the brominated oligonucleotide, SS_1-AB*, was hybridized to a semicomplementary oligonucleotide, SS_4-CC, resulting in a 5 bp mismatched bubble, the level of strand breaks was approximately the same as in the single-stranded DNA except that new products, consisting of interstrand cross-links, appeared as high-molecular weight bands in the denaturing gels ($DBsc_{1/4}$-AB*//CC, lanes 12−15).

Wavelength Dependence of Strand Break and ICL Formation in Brominated Complementary (Figure 4) or Semicomplementary (Figure 5) Double-Stranded DNA. The presence of bromodeoxyuridine in the complementary double-stranded oligonucleotide (Figure 4, $DBc_{1/3}$-AB*//TA) greatly enhances UV-induced strand breakage for each studied wavelength. We observe a maximum of strand breaks near 280 nm (Figure 4, lanes 9−13) but almost no production of ICL at this or any studied wavelength.

The presence of bromodeoxyuridine within a single-stranded bubble in the semicomplementary double-stranded oligonucleotide (Figure 5, $DBsc_{1/4}$-AB*//CC) suppressed UV-induced strand breakage for all studied wavelengths, compared to that of fully duplex brominated DNA. However, substantial ICL production was observed for each wavelength (ICL zone, Figure 5). We observe a maximum of ICL and strand break formation near 280 nm (Figure 5, lanes 9−13).

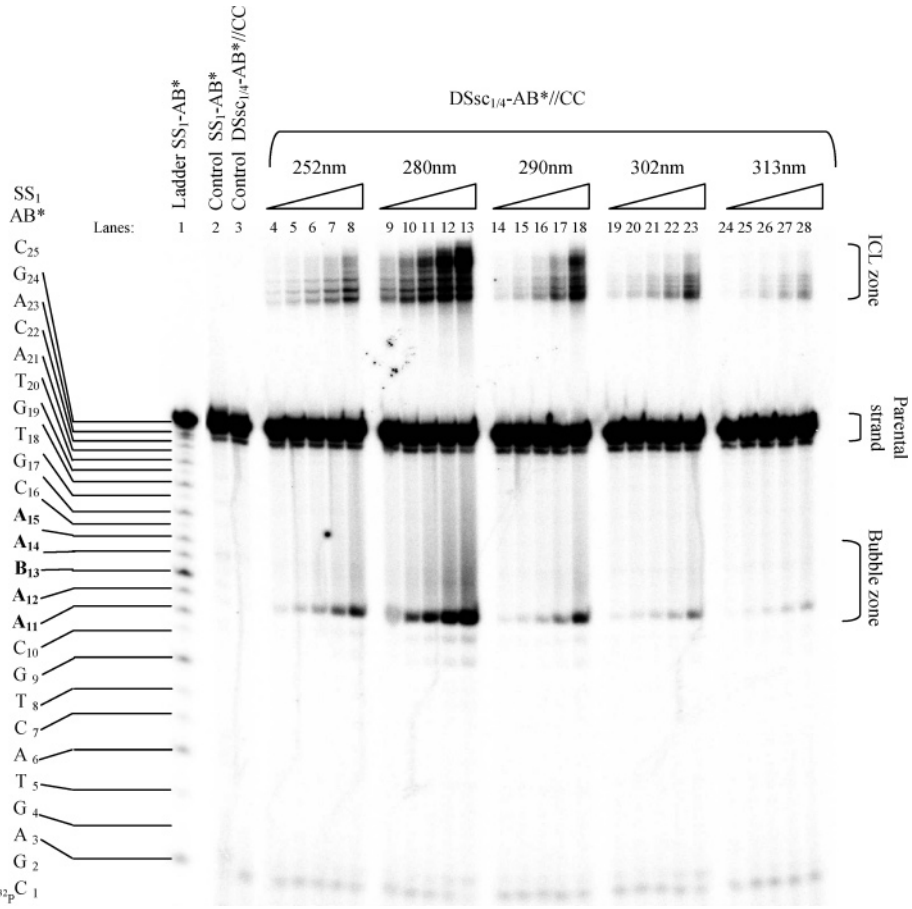

FIGURE 5: Formation of single-strand breaks and interstrand cross-links in bromodeoxyuridine-sensitized oligonucleotides. Oligonucleotides were UV-irradiated with different doses (see legend of Figure 4) and wavelengths (252, 280, 290, 302, and 313 nm) under a nitrogen atmosphere, and damage in a double-stranded oligonucleotides with a single-stranded bubble ($DSsc_{14}$-AB*//CC) (nucleotides 11−15 mismatched) was assessed. The asterisk indicates the ^{32}P-labeled strand. In this experiment, the strand containing a BrdUrd (oligonucleotide SS_1-AB) at position 13 was labeled with ^{32}P.

Quantum Yields for Strand Break and Interstrand Cross-Link Formation for Different Wavelengths and DNA Secondary Structures (Figure 6a,b). Figure 6 shows the quantum yield of strand breaks (panel a) and interstrand cross-links (panel b) for each DNA structure (SS, DSc, and DSsc) for the brominated (SS_1-AB*) and nonbrominated oligonucleotide (SS_2-AT*).

Only brominated duplex DNA gives efficient production of single-strand breaks [Figure 6a, $DSc_{1/3}$-AB*//TA (□)] with a maximum quantum yield near 280 nm. For the brominated complementary double-stranded DNA, the maximum quantum yield is 0.06; i.e., ∼16 absorbed photons are required to produce one strand break.

In the case of ICL, a maximum quantum yield for each DNA structure for both the brominated and the nonbrominated strands occurs near 280 nm. The ideal condition for the production of ICL is when the BrdUrd is present within the bubble zone [$DSsc_{1/4}$-AB*//CC (△)]. Interestingly, a substantial but less important production of ICL is obtained when two nonbrominated strands are hybridized to form a semicomplementary oligonucleotide containing a 5 bp mismatched bubble [$DSsc_{2/3}$-AT*//CC (▲)]. A weak production of ICL is also obtained with brominated complementary double-stranded DNA [$DSc_{1/3}$-AB*//TA (□)], but no ICL were detected for nonbrominated complementary DNA.

Wavelength Specificity for Strand Break and ICL Formation in Nonbrominated Semicomplementary (Figure 6c) Double-Stranded DNA. Figure 6c shows the quantum yield of strand breaks (dashed line) and interstrand cross-links (solid line) for the nonbrominated complementary (SS_3-TA*) or semicomplementary strand (SS_4-CC*) and for oligonucleotides hybridized with a brominated oligonucleotide (SS_1-AB). As expected, the quantum yield for ICL formation is independent of the identity of the labeled strand. Nevertheless, strand breaks are observed in the nonbrominated strand when hybridized with a brominated strand to form a bubble zone, whereas no detectable strand breaks are observed when a nonbrominated strand is hybridized with a brominated strand to form a completely double-stranded DNA.

Influence of BrdUrd on Strand Break Formation by UVB Irradiation in a pGEM Plasmid. The induction of DNA strand breaks by UVB (302 nm) in brominated and nonbrominated pGEM-3Zf(−) plasmid is shown Figure 7. Irradiation of brominated plasmid leads to the loss of the supercoiled form and to the formation of relaxed circular (R) molecules. A dose of 80 kJ/m^2 converted 83% of the supercoiled plasmid to the relaxed circular form, while under the same conditions, no damage was detectable in the nonbrominated plasmid.

Wavelength Dependence of Strand Break Formation in a BrdUrd-Substituted pGEM Plasmid. Figure 8 shows the wavelength dependence for strand breakage in brominated and nonbrominated pGEM near 280, 302, and 313 nm. The efficiency of strand breakage was maximal near 280 nm.

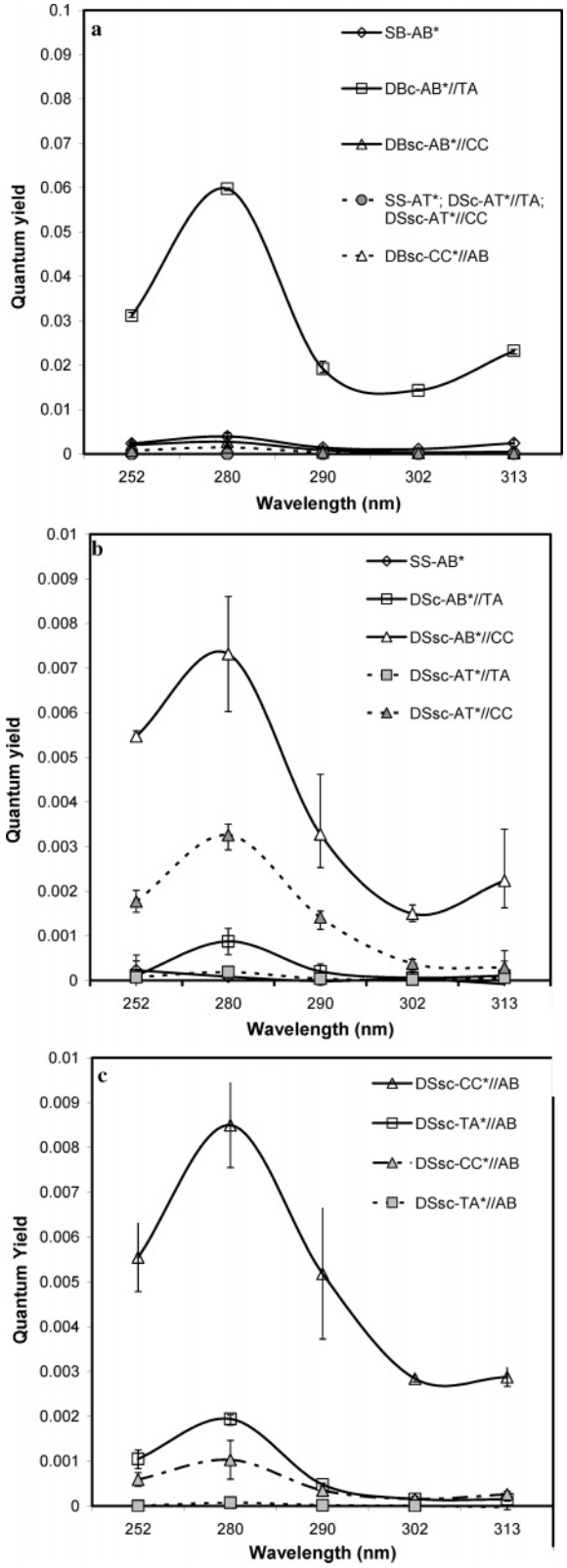

FIGURE 6: (a) Quantum yields of ICL in brominated or nonbrominated DNA as a function of the wavelengths of UV irradiation (252, 280, 290, 302, and 313 nm) and the structure of the DNA (SS, DSc, and DSsc). (b) Quantum yields of strand breaks in brominated and nonbrominated DNA as a function of the wavelengths of UV irradiation (252, 280, 290, 302, and 313 nm) and the structure of the DNA (SS, DSc, and DSsc). (c) Quantum yields of ICL and strand breaks in the nonbrominated complementary or semicomplementary strand hybridized with a brominated strand, as a function of the wavelength of UV irradiation (252, 280, 290, 302, and 313 nm) and DNA structure (SS, DSc, and DSsc).

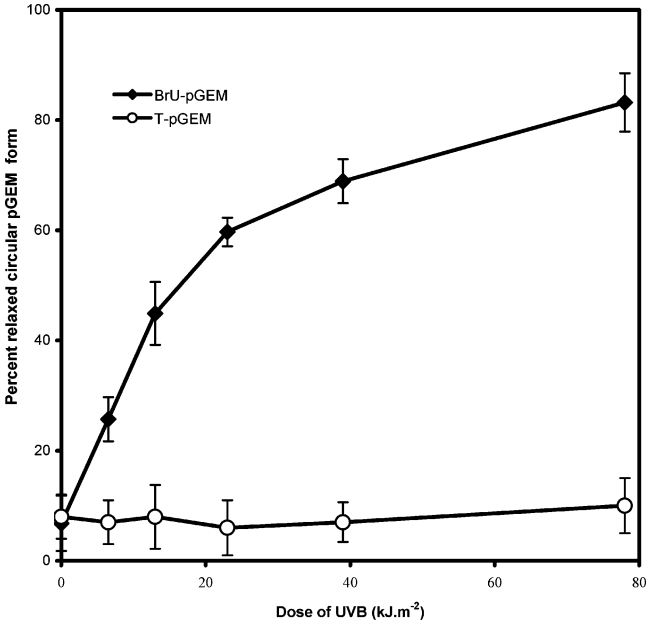

FIGURE 7: Induction of single-strand breaks in plasmid DNA by UV irradiation as a function of dose. Brominated (◆, BrU-pGEM) and nonbrominated (○, T-pGEM) plasmid were irradiated with UVB using a transilluminator, and the yields of the relaxed circular form were quantified. Bars represent standard errors.

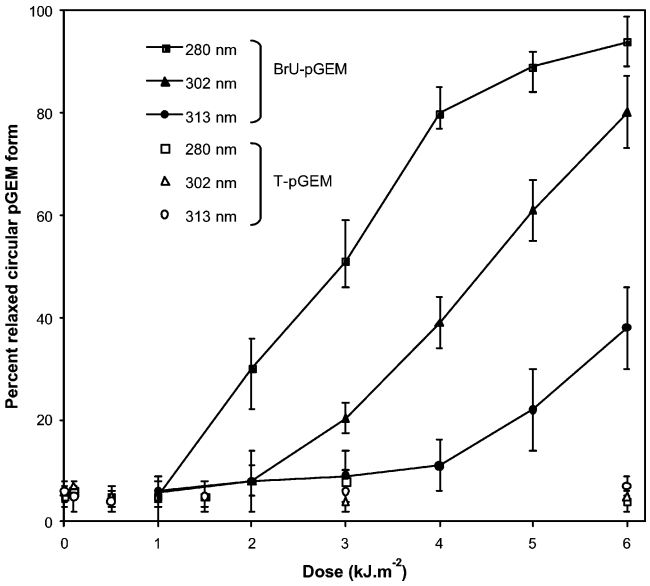

FIGURE 8: Induction of single strand breaks in plasmid DNA by UVB radiation (280, 302, and 313 nm). Brominated (Br) and nonbrominated (NBr) plasmids were irradiated, and the yields of the relaxed circular form were quantified. Bars represent standard errors.

Under the same conditions, no detectable damage was observed in nonbrominated plasmid (empty symbols in Figure 8).

DNA ICL Formation in Supercoiled Brominated Plasmid DNA. The negatively supercoiled form of DNA is more prone to breathing or even denaturing in AT-rich regions than the linear form. Thus, on the basis of our results with oligonucleotides, one would expect supercoiling to enhance ICL production during UV irradiation. To test this hypothesis, interstrand cross-link production in supercoiled and linear plasmids by UVB irradiation was investigated using an

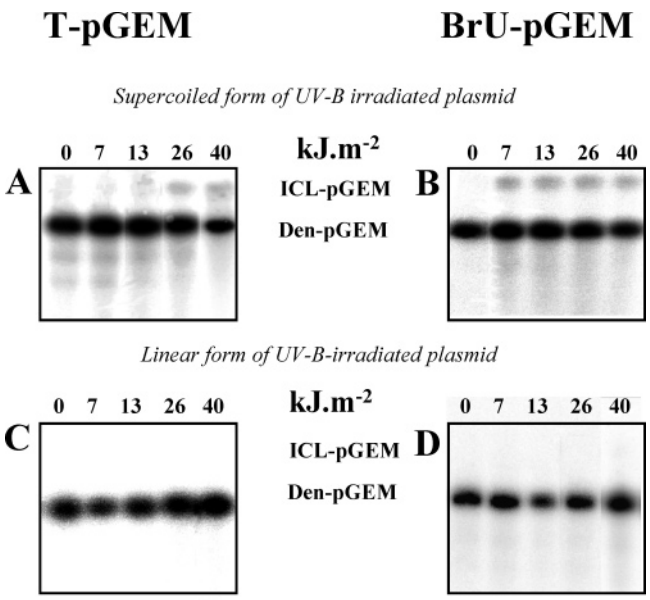

FIGURE 9: Alkaline agarose gel showing ICL DNA in nonbrominated and brominated plasmids. The ICL DNA (ICL-pGEM) has a lower electrophoretic mobility than denatured (Den-pGEM) single-stranded DNA (A and B). In parallel, the plasmid was digested with *Hin*dIII before UVB irradiation (C and D). Panels A and C contained nonbrominated DNA and panels B and D brominated DNA.

alkaline agarose gel electrophoresis assay (Figure 9). Two bands are present: a major, fast-migrating band corresponding to the denaturation of nicked plasmid (ss-pGEM) and a second, less intense, slower-migrating band (ICL-pGEM), resulting from one or more ICLs. This latter band (ICL-pGEM) can only be observed when the supercoiled form of brominated or nonbrominated pGEM is UVB irradiated. Figure 9B shows that no ICL DNA is produced when the linear form of brominated or nonbrominated pGEM is UVB irradiated.

DISCUSSION

We have previously hypothesized that radiosensitization of DNA by BrdUrd is most important in open DNA bubble regions which exist under several physiological situations. In these regions, the proximity of the opposite, nonbrominated strand as well as the mobility of the bases in the single-stranded bubble allows the uridin-5-yl radical, formed during γ irradiation by the interaction of an aqueous electron and BrdUrd, to damage bases on the same or the opposite strand and thus to distribute the damage, albeit unequally, between both strands (*26*). In addition, interstrand cross-links are formed in these bubble regions (*27*). In the work presented here, we investigated the formation of damage in both normal and BrdUrd-substituted DNA as a function of the UV irradiation wavelength and the secondary structure of the DNA, with the goal of comparing the products and the underlying mechanisms involved in strand break and ICL formation for UV and ionizing radiation.

Our Model of Open DNA: The Bubble. The DNA bubble in our model system consists of five mismatched bases in the center of a 25 bp double-stranded oligonucleotide, with the BrdUrd at position 13 (Figure 1). Thus, the bases on the opposite strands of the single-stranded bubble are much more mobile than their base-paired neighbors but are still constrained to remain in proximity by the flanking double-stranded portions of the oligonucleotide. This greater mobility confers some single-strand properties to these bases (*20*), thus allowing the formation of either an intercalation structure or an open region (*28*, *29*). This mobility could explain a change in the fate of intermediate uracil-5-yl radicals from a pathway that leads to H-atom abstraction and strand cleavage to a pathway that reacts with adjacent bases and produces ICL.

DNA Strand Break Formation. It is well-known that DNA strand breakage induced by UV irradiation of brominated DNA arises from electron transfer between an adjacent adenine and the BrdUrd. The formation of stable products from initial transfer depends on several factors, such as forward and back electron transfer rates, radical cation migration, and probably base stacking (*30*−*32*). Some studies have already shown that radical cation migration along the DNA is suppressed by the presence of mismatched bases or low-energy well traps in the path of migration (*33*, *34*). It is evident that base stacking, hydrogen bonding between bases, the presence of metal cations, and the degree of solvatation can contribute greatly to the conversion of DNA radicals to damage (*35*, *36*). In this study, we demonstrate that the conformation and the flexibility of brominated DNA greatly influence the quantity and the quality of damage induced by BrdUrd photolysis.

We observe, in agreement with other studies, that DNA strand break formation in the brominated strand is greatly enhanced in complementary double-stranded DNA, and is quenched in single-stranded and semicomplementary double-stranded DNA. Interestingly, no DNA strand breaks were observed in the complementary nonbrominated strand perfectly hybridized with a brominated strand; however, breaks in the semicomplementary nonbrominated strand were observed when it was hybridized with a brominated strand to form a single-stranded zone around the BrdUrd. The maximum level of strand break formation for all these conditions is near 280 nm. Thus, depending on the structure of the DNA, BrdUrd can greatly enhance breakage of only the brominated strand, in completely duplex-brominated DNA, or both the brominated and nonbrominated strands in the case of semicomplementary DNA.

DNA Cross-Links. Until recently, intrastrand cross-links between two adjacent nonbrominated pyrimidines and DNA strand breakage in brominated DNA were thought to be the most toxic DNA lesions produced by UV irradiation. However, Kypr's group has recently demonstrated that UVC light can induce interstrand cross-links (*7*−*9*) between the complementary strands of DNA without chemical agents. In addition, Cadet et al. have shown that UVC can create an ICL in A-form DNA and have characterized this ICL lesion by mass spectroscopy (*10*). They found that thymines on opposite strands form an ICL, essentially a spore photoproduct, within dry DNA irradiated with UVC. Dehydration either by lyophilization or by addition of a dehydrating agent such as alcohol was essential for ICL formation. We demonstrate here that production of ICL is greatly enhanced by the presence of BrdUrd within a 5 bp mismatch flanked by double-stranded B-form DNA.

The mechanism of UV-induced damage of DNA containing BrdU appears to involve two initial reactions of excited BrdUrd (*18*, *37*). The well-known pathway of halogenated

compounds involves cleavage of the homolytic C−Br bond of excited BrdUrd leading to intermediate deoxyuridin-5-yl radicals. These radicals can subsequently abstract H-atoms from either the C1′ or C2′ position of the deoxyribose moiety, although the reaction is complicated by the possible rearrangement of sugar radicals (*38*). Another pathway involves photoinduced electron transfer from the adjacent base to excited BrdUrd, which generates a radical ion pair. BrdU radical anions subsequently lose Br anions to give deoxyuridin-5-yl radicals. Thus, the damaging radical species in both the homolytic cleavage and electron transfer-mediated pathways is likely deoxyuridin-5-yl radicals. A major difference between the two pathways however is that electron transfer produces base radical cations. The latter radicals appear to participate in the overall reaction first by enhancing the rate of H-atom abstraction from C1′ by deoxyuridin-5-yl radicals and second by acting as an oxidizing agent for subsequently formed sugar radicals, thereby converting them to carbocations. Interestingly, electron transfer to excited BrdUrd occurs only when there is a flanking 5′-adenine residue. For example, the presence of guanine, thymine, and cytosine, in place of adenine, greatly reduces the extent of strand cleavage in specific oligonucleotides (*39*, *40*). Inhibition of electron transfer in DNA in which dGuo was adjacent to BrdUrd has been attributed to rapid recombination of initial radical ion pairs (*40*).

Electron transfer is probably the most important pathway leading to DNA damage in UV-irradiated DNA containing BrdUrd. This is consistent with the more efficient formation of direct strand breaks in UV-irradiated double-stranded DNA compared to single-stranded DNA (*41*). Initial electron transfer will be favored in double-stranded DNA because of overlap of the π orbitals of BrdUrd and dAdo. In addition, electron transfer induces more direct cleavage of DNA because radical cations of dAdo facilitate H-atom abstraction and the formation of cleavage products (*42*). In contrast, the formation of breaks by the reaction of solvated electrons, generated by ionizing radiation, with DNA containing BrdUrd is more efficient in single-stranded DNA than in double-stranded DNA (*26*). In this case, the capture and loss of the bromine anion lead exclusively to deoxyuridin-5-yl radicals. Thus, the low yield of breaks in double-stranded DNA is likely due to electron transfer of BrdUrd radical anions to other bases.

The presence of a bubble region within double-stranded DNA leads to a decrease in the level of direct cleavage of DNA, with an increase in the level of formation of novel interstrand cross-links. The formation of these products indicates a change in the mechanism of DNA damage in single-stranded regions of double-stranded DNA. One possibility is that the reactivity of excited BrdUrd within the bubble is similar to that in single-stranded DNA. On the other hand, one cannot rule out electron transfer within the bubble because the helix structure will largely be conserved within this 5 bp region, and thus, π-stacking interactions should still occur between adjacent bases. The formation of novel products within the bubble indicates that the chemistry of initial species, i.e., deoxyuridin-5-yl radicals, is diverted from reaction with the deoxyribose moiety on the same strand to reaction with DNA bases on the opposite strand. Previous studies suggest that oxygen can react with deoxyuridin-5-yl radicals and thereby compete with H-atom abstraction on the same strand. Moreover, cross-link products between BrdUrd and pyrimidines have been observed in UV photolysis of hexanucleotides (*42*). The presence of a bubble within double-stranded DNA provides a new environment in which the radicals of one strand can favorably react with base and perhaps sugar moieties of the other strand. These reactions will not occur in single-stranded DNA because the reactants are too dilute in solution to compete with H-atom abstraction. Thus, the mechanism of cross-link formation in bubbles involves the formation of deoxyuridin-5-yl radicals by either homolytic cleavage or electron transfer, followed by addition of these radicals to base moieties on the opposite strand. In the case of electron transfer, the adduct radical of deoxyuridin-5-yl radicals and pyrimidines may undergo oxidation by the adenine radical cation to directly give diamagnetic products.

Differences between BrdUrd Degradation by UV or γ Irradiation. We have proposed that the anionic complex formed by an electron and BrdUrd during γ irradiation of the nucleoside, either free or incorporated into single-stranded DNA, is probably stabilized by delocalization of the charge into the aromatic ring and by the electroaffinity of the bromine atom leading to the break of the C−Br bond (*26*, *27*). However, this electrophilic property of the bromine atom decreases in more complex conjugated systems (*43*) such as the BrdUrd·deoxyadenosine base pair in double-stranded DNA, allowing delocalization of the excess electron toward adenine and onto the oxygen involved in hydrogen bonding. We have supposed that fewer uridine-yl radicals are formed in double-stranded DNA than in single-stranded DNA as a result of electron transfer to other bases or the medium. In the work presented here, UV irradiation leads to more strand breaks in brominated double-stranded DNA than in brominated double-stranded DNA containing a bubble. These results may initially appear to be in contradiction to those obtained with γ irradiation in which double-stranded DNA is resistant to strand break formation compared to single-stranded DNA (*26*). For both types of radiation, an additional electron is added to the BrdUrd leading to the formation of a transitory anion $[BrdUrd]^-$. In γ and UV irradiation, the behavior of this anion is highly dependent on the structure of the DNA; in the case of γ radiation, there is more release of Br^- and strand break formation in a semicomplementary double-stranded DNA (*26*), whereas in UV irradiation, there is more release of Br^- and strand break formation in a complementary double-stranded DNA. The C−Br bond is already weakened by the UV photon absorbed; the presence of the additional electron will further weaken the C−Br bond leading to the release of Br^- (*44*, *45*). In double-stranded DNA, the newly formed uracilyl can abstract an H1′ or H2′ from the sugar to yield a radical centered on C1′ or C2′ of deoxyribose. The radical, localized on the sugar, can lead to base release or a DNA strand break, respectively. In semicomplementary double-stranded DNA, the uracilyl radical can equally abstract hydrogen from the sugar moiety; however, under these conditions, the uracilyl radical has more mobility than in double-stranded DNA, and the abstraction of hydrogen can occur on nearby bases of the same strand or bases or even the sugar moiety of the opposite strand. In both γ and UV irradiation, the quantity of electrons that are available to interact with the BrdUrd is a crucial parameter. Thus, in the case of γ radiation, oxygen and other molecules

can quench solvated electrons, while in UV photolysis, the presence of the bubble can perturb the transfer of charge along the DNA, thus reducing the chance of an electron reaching the excited BrdUrd.

Thus, our results with UV radiation are consistent with those obtained with γ radiation, and in addition, they demonstrate that when the uracilyl radical is produced in double-stranded DNA, the strand break will occur on the same strand as the radical.

Biological Implications of Our Results. We propose that UV radiation of cells containing BrdUrd incorporated randomly into duplex DNA will create many ssb, whereas BrdUrd present in DNA bulges or open regions in double-stranded DNA (transcription bubbles, replication forks) will lead to damage in both strands in the form of ICL. These findings may help explain the potent clinical antiviral activity of IdUrd and BrdUrd and suggest that ICL formation may be a very specific probe for identifying single-stranded regions in the DNA of living cells. In addition, this model system provides an excellent means of introducing ICL for studies on their repair or biological consequences.

REFERENCES

1. Cole, S. (1973) Repair of DNA containing interstrand cross-links in *Escherichia coli*: Sequential excision and recombination, *Proc. Natl. Acad. Sci. U.S.A. 69*, 1064−1068.
2. Berardini, M., Mackay, W., and Loechler, E. L. (1997) A site-specific study of a plasmid containing single nitrogen mustard interstrand cross-link: Evidence for a second, recombination independent pathway for the DNA repair of interstrand cross-links, *Biochemistry 36*, 3506−3513.
3. Sasaki, M. S., Takata, M., Sonoda, E., Tachibana, A., and Takeda, S. (2004) Recombination repair pathway in the maintenance of chromosomal integrity against DNA interstrand crosslinks, *Cytogenet. Genome Res. 104*, 28−34.
4. Rothfuss, A., and Grompe, M. (2004) Repair kinetics of genomic interstrand DNA cross-links: Evidence for DNA double-strand break-dependent activation of the Fanconi anemia/BRCA pathway, *Mol. Cell. Biol. 24*, 123−134.
5. Pichierri, P., Averbeck, D., and Rosselli, F. (2002) DNA cross-link-dependent RAD50/MRE11/NBS1 subnuclear assembly requires the Fanconi anemia C protein, *Hum. Mol. Genet. 11*, 2531−2546.
6. Zhen, W., Evans, M. K., Haggerty, C. M., and Bohr, V. A. (1993) Deficient gene specific repair of cisplatin-induced lesions in *Xeroderma pigmentosum* and Fanconi's anemia cell lines, *Carcinogenesis 14*, 919−924.
7. Najedly, K., Kittner, R., Pospisilova, S., and Kypr, J. (2001) Crosslinking of the complementary strands of DNA by UV light: Dependence on the oligonucleotide composition of the UV irradiated DNA, *Biochim. Biophys. Acta 1517*, 365−375.
8. Pospisilova, S., and Kypr, J. (1997) UV light-induced crosslinking of the complementary strands of plasmid pUC19 DNA restriction fragments, *Photochem. Photobiol. 65*, 945−948.
9. Nejedly, K., Kittner, R., and Kypr, J. (2001) Genomic DNA regions whose complementary strands are prone to UV light-induced crosslinking, *Arch. Biochem. Biophys. 388*, 216−224.
10. Douki, T., Laporte, G., and Cadet, J. (2003) Inter-strand photoproducts are produced in high yield within A-DNA exposed to UVC radiation, *Nucleic Acids Res. 31*, 3134−3142.
11. Dewey, W. C., and Humphrey, R. M. (1965) Increase in radiosensitivity to ionizing radiation related to replacement of thymidine in mammalian cells with 5-bromodeoxyuridine, *Radiat. Res. 26*, 538−553.
12. Sano, K., Hoshino, T., and Nagai, M. (1968) Radiosensitization of brain tumor cells with a thymidine analogue (bromouridine), *J. Neurosurg. 28*, 530−538.
13. Webb, C. F., Jones, G. D., Ward, J. F., Moyer, D. J., Aguilera, J. A., and Ling, L. L. (1993) Mechanisms of radiosensitization in bromodeoxyuridine-substituted cells. *Int. J. Radiat. Biol. 64*, 695−705.
14. Ling, L. L., and Ward, J. F. (1990) Radiosensitization of Chinese hamster V79 cells by bromodeoxyuridine substitution of thymidine: Enhancement of radiation-induced toxicity and DNA strand break production by monofilar and bifilar substitution, *Radiat. Res. 121*, 76−83.
15. Taguchi, T., and Shiraishi, Y. (1989) Increased sister-chromatid exchanges (SCEs) and chromosomal fragilities by BrdU in a human mutant B-lymphoblastoid cell line, *Mutat. Res. 211*, 43−49.
16. Ribas, M., Korenberg, J. R., Peretti, D., Pichiri, G., Stockert, J. C., Gosalvez, J., and Mezzanotte, R. (1994) Sister chromatid differentiation in 5-bromo-2′-deoxyuridine-substituted chromosomes: A study with DNA-specific ligands and monoclonal antibody to histone H2B, *Chromosome Res. 2*, 428−438.
17. Wojcik, A., von Sonntag, C., and Obe, G. (2003) Application of the biotin-dUTP chromosome labelling technique to study the role of 5-bromo-2′-deoxyuridine in the formation of UV-induced sister chromatid exchanges in CHO cells, *J. Photochem. Photobiol., B 69*, 139−144.
18. Sugiyama, H., Tsutsumi, Y., and Saito, I. (1990) Highly sequence-selective photoreaction of 5-bromouracil-containing deoxyhexanucleotides, *J. Am. Chem. Soc. 112*, 6720−6721.
19. Zeng, Y., and Wang, Y. (2004) Facile Formation of an Intrastrand Cross-Link Lesion between Cytosine and Guanine upon Pyrex-Filtered UV Light Irradiation of d(^{Br}CG) and Duplex DNA Containing 5-Bromocytosine, *J. Am. Chem. Soc. 126*, 6552−6553.
20. Bhattacharyya, A., and Lilley, D. M. (1989) The contrasting structures of mismatched DNA sequences containing looped-out bases (bulges) and multiple mismatches (bubbles), *Nucleic Acids Res. 17*, 6821−6840.
21. Gamber, H., Piette, J., and Hearst, J. E. (1984) Efficient formation of a crosslinkable HMT monoadduct at the Kpn I recognition site, *Photochem. Photobiol. 40*, 29−34.
22. Teng, S. P., Woodson, S. A., and Crothers, D. M. (1989) DNA sequence specificity of mitomycin cross-linking, *Biochemistry 28*, 3901−3907.
23. Millard, J. T., Weidner, M. F., Kirchner, J. J., Ribeiro, S., and Hopkins, P. B. (1991) Sequence preferences of DNA interstrand crosslinking agents: Quantitation of interstrand crosslink locations in DNA duplex fragments containing multiple crosslinkable sites, *Nucleic Acids Res. 19*, 1885−1891.
24. Martin, F., Burrow, P. D., Cai, Z., Cloutier, P., Hunting, D. J., and Sanche, L. (2004) DNA strand breaks induced by 0−4 eV electrons: The role of shape resonances, *Phys. Rev. Lett. 93*, 068101-1-4.
25. Sambrook, J., and Russell, D. W. (2001) *Molecular Cloning*, 3rd ed., Vol. 1, Cold Spring Harbor Laboratory Press, Plainview, NY.
26. Cecchini, S., Girouard, S., Huels, M. A., Sanche, L., and Hunting, D. J. (2004) Single strand specific radiosensitization of DNA by bromodeoxyuridine, *Radiat. Res. 162*, 604−615.
27. Cecchini, S., Girouard, S., Huels, M. A., Sanche, L., and Hunting, D. J. (2005) Interstrand cross-links: A new type of γ ray damage in bromodeoxyuridine substituted DNA, *Biochemistry 44*, 1932−1940.
28. Chou, S.-H., Chin, K. H., and Wang, A. H. (2003) Unusual DNA duplex and hairpin motifs, *Nucleic Acids Res. 31*, 2461−2474.
29. Shepard, W., Cruse, W. B., Fourme, R., de la Fortelle, E., and Prange, T. (1998) A zipper-like duplex in DNA: The crystal structure of d(GCGAAAGCT) at 2.1 Å resolution, *Structure 6*, 849−861.
30. Colson, A. O., and Sevilla, M. D. (1995) Elucidation of primary radiation damage in DNA through application of ab initio molecular orbital theory, *Int. J. Radiat. Biol. 67*, 627−645.
31. Hutter, M., and Clark, T. (1996) On the Enhanced Stability of the Guanine-Cytosine Base-Pair Radical Cation, *J. Am. Chem. Soc. 118*, 7574−7577.
32. Saito, I., Nakamura, T., Nakatani, K., Yoshioka, Y., Yamaguchi, K., and Sugiyama, H. (1998) Mapping of the Hot Spots for DNA Damage by One-Electron Oxidation: Efficacy of GG Doublets and GGG Triplets as a Trap in Long-Range Hole Migration, *J. Am. Chem. Soc. 120*, 12686−12687.
33. Kelley, S. O., Boon, E. M., Barton, J. K., Jackson, N. M., and Hill, M. G. (1999) Single-base mismatch detection based on charge transduction through DNA, *Nucleic Acids Res. 27*, 4830−4837.
34. Okada, A., Yokojima, S., Kurita, N., Sengoku, Y., and Tanaka, S. (2003) Charge transfer in duplex DNA containing mismatch, *THEOCHEM 630*, 283−290.
35. Falcone, J. M., Becker, D., Sevilla, M. D., and Swarts, S. G. (2005) Products of the reactions of the dry and aqueous electron with

hydrated DNA: Hydrogen and 5,6-dihydropyrimidines, *Radiat. Phys. Chem. 72*, 257−264.
36. Ambroz, H. B., Kemp, T. J., Rodger, A., and Przybytniak, G. (2004) Ferric and ferrous ions: Binding to DNA and influence on radiation-induced processes, *Radiat. Phys. Chem. 71*, 1023−1030.
37. Cook, G. P., and Greenberg, M. M. (1996) A Novel Mechanism for the Formation of Direct Strand Breaks upon Anaerobic Photolysis of Duplex DNA Containing 5-Bromodeoxyuridine, *J. Am. Chem. Soc. 118*, 10025−10030.
38. Sugiyama, H., Fugimoto, K., and Saito, I. (1996) Evidence for intrastrand C2′ hydrogen abstraction in photoirradiation of 5-halouracil-containing oligonucleotides by using stereospecifically C2′-deuterated deoxyadenosine, *Tetrahedron Lett. 37*, 1805−1808.
39. Ito, T., and Rokita, S. E. (2004) Reductive Electron Injection into Duplex DNA by Aromatic Amines, *J. Am. Chem. Soc. 126*, 15552−15559.
40. Chen, T., Cook, G. P., Koppisch, A. T., and Greenberg, M. M. (2000) Investigation of the Origin of the Sequence Selectivity for the 5-Halo-2′-deoxyuridine Sensitization of DNA to Damage by UV-Irradiation, *J. Am. Chem. Soc. 122*, 3861−3866.
41. Cook, G. P., Chen, T., Koppisch, A. T., and Greenberg, M. M. (1999) The effects of secondary structure and O_2 on the formation of direct strand breaks upon UV irradiation of 5-bromodeoxyuridine-containing oligonucleotides, *Chem. Biol. 6*, 451−459.
42. Hatano, K., Sugiyama, H., and Saito, I. (1995) Photoreaction of 5′-halouracil-containing DNA. A novel photoproduct at 5′BrU-pyrimidine-3′ sequence, *Nucleic Acids Symp. Ser. 34*, 31−32.
43. Li, X., Sevilla, M. D., and Sanche, L. (2003) Density Functional Theory Studies of Electron Interaction with DNA: Can Zero eV Electrons Induce Strand Breaks? *J. Am. Chem. Soc. 125*, 8916−8920.
44. Dietz, T. M., Von Trebra, R. J., Swanson, B. J., and Koch, T. H. (1987) Photochemical coupling of 5-bromouracil (BU) to a peptide linkage. A model for BU-DNA protein photocrosslinking, *J. Am. Chem. Soc. 109*, 1793−1797.
45. Ito, S., Saito, I., and Matsuura, T. (1980) Acetone-sensitized photocoupling of 5-bromouridine to tryptophan derivatives via electron-transfer process, *J. Am. Chem. Soc. 102*, 7535−7541.

BI050799X